Planetary and Space Science 209 (2021) 105372

Contents lists available at ScienceDirect

Planetary and Space Science

journal homepage: www.elsevier.com/locate/pss

Tintigny meteorite: the first Belgian achondrite

Hamed Pourkhorsandi [a,*], Vinciane Debaille [a], Jérôme Gattacceca [b], Richard Greenwood [c], Thierry Leduc [d], Marleen De Ceukelaire [d], Sophie Decrée [d], Steven Goderis [e]

[a] Laboratoire G-Time, Université Libre de Bruxelles, CP 160/02, 50, Av. F.D. Roosevelt, 1050, Brussels, Belgium
[b] CNRS, Aix-Marseille Univ, IRD, INRAE, CEREGE, Aix-en-Provence, France
[c] School of Physical Sciences, The Open University, Walton Hall, Milton Keynes, MK7 6AA, United Kingdom
[d] Royal Belgian Institute of Natural Sciences, Geological Survey of Belgium, 1000, Brussels, Belgium
[e] Department of Chemistry, Research Unit: Analytical, Environmental and Geo-Chemistry, Vrije Universiteit Brussel, Brussels, 1050, Belgium

ARTICLE INFO

Keywords:
Achondrite
Fall
Eucrite
Belgium
Tintigny

ABSTRACT

A late afternoon in February 1971, a meteorite impacted the rooftop of a house in Tintigny village in southern Belgium. Confirmed as a possible meteorite by the schoolteacher, the meteorite and its fall story did not leave the village. Finally, 46 years after the fall event, we got the opportunity to study and characterize this meteorite. In this work, we give a detailed report on its textural, mineralogical, whole-rock elemental and oxygen isotopic composition. Officially named as Tintigny, we classified it as an achondrite from howardite-eucrite-diogenite (HED) clan and more precisely a polymict eucrite. A brecciated basaltic rock believed to be originated from the surface of V-type asteroids namely the asteroid 4 Vesta. Tintigny has recorded the evidence of the impact metamorphism and metasomatism processes active on its parent body. Tintigny is one of the 39 eucrite falls known to date, and one of the 11 eucrites occurred in Europe. It is the fifth officially recognized meteorite and the first achondrite from Belgium. This report shows the importance of studying and accessing such a meteorite for further cosmochemical and planetary investigations and enriching our knowledge on the formation of HED meteorites and their parent bodi(es). In addition, it brings the attention to its importance as a scientific heritage that has to be properly understood and safeguarded for the generations of scientists, scholar, and amateurs to come.

1. Introduction

In February 1971 (precise date not recorded), Mr Eudore Schmitz was working in his barn in the village of Tintigny (southern Belgium, 49.683786°N, 5.532957°E) during the late afternoon when he heard a loud noise from the roof of the building. After going upstairs, he found a hole in a tile and a black stone on the barn floor. It was suggested that he burnt himself picking up the fragment, so he used some hay and then his hat to hold the stone. The schoolteacher of the village, Mr Albert Rossignon, confirmed that the stone was a meteorite and kept it, hoping that his identification would be confirmed during a subsequent investigation. The teacher later joined a religious seminary and became a priest. While he faithfully kept the meteorite and showed it from time to time to visitors and children, the stone and associated story never left the region. In 2017, after reading an article about recent Belgian meteorite recovery expeditions in Antarctica, he contacted Dr Vinciane Debaille, professor at the Université Libre de Bruxelles (ULB) and specialist in planetary sciences and meteoritics who recognized the stone as an achondritic meteorite. The meteorite was subsequently donated by Madam Germaine Mathus, widow of Mr Eudore Schmitz, and her children, Jean-Paul, Rita and Joseph Schmitz, to the Royal Belgian Institute for Natural Science (RBINS) and studied. While the meteorite is no longer complete due to handling of the stone by various people over the years, Father Rossignon affirms that the fusion crust was initially complete, with a piece of the tile originally stuck on the stone.

We have classified this meteorite as a polymict eucrite and Tintigny, its official name, has been approved by the Nomenclature Committee of the Meteoritical Society (Gattacceca et al., 2020). Tintigny is the fifth officially recognized meteorite and the first achondrite from the Belgian territory (Fig. 1). This meteorite is now on permanent open display at RBINS.

In this paper, details on the petrological, geochemical, and isotopic characteristics of Tintigny are reported and its formation processes studied.

* Corresponding author.
E-mail address: hamed.pourkhorsandi@ulb.ac.be (H. Pourkhorsandi).

https://doi.org/10.1016/j.pss.2021.105372
Received 19 March 2021; Received in revised form 18 October 2021; Accepted 27 October 2021
Available online 29 October 2021
0032-0633/© 2021 Elsevier Ltd. All rights reserved.

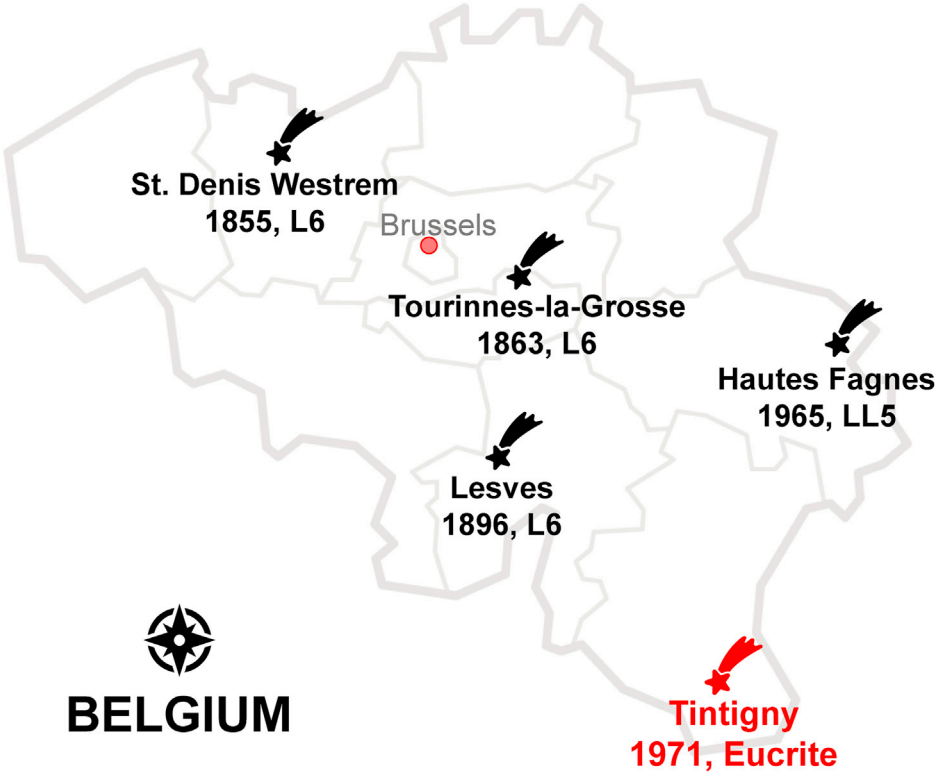

Fig. 1. Meteorites of Belgium with fall/find years and types.

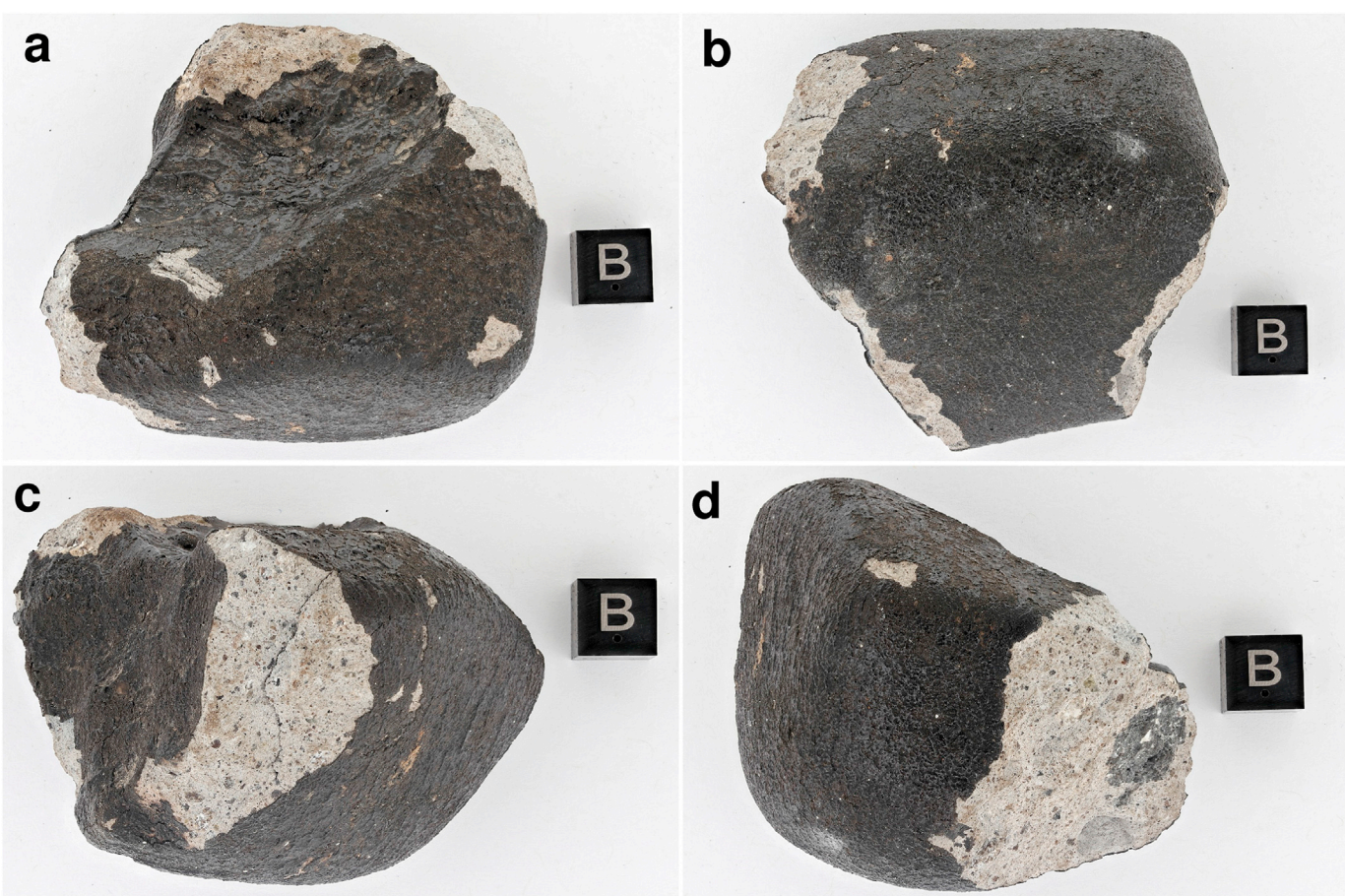

Fig. 2. Tintigny meteorite from different angles. Note the different textures of fusion crust, the occurrence of fractures, and a dark grey clast in d. Image credit: RBINS.

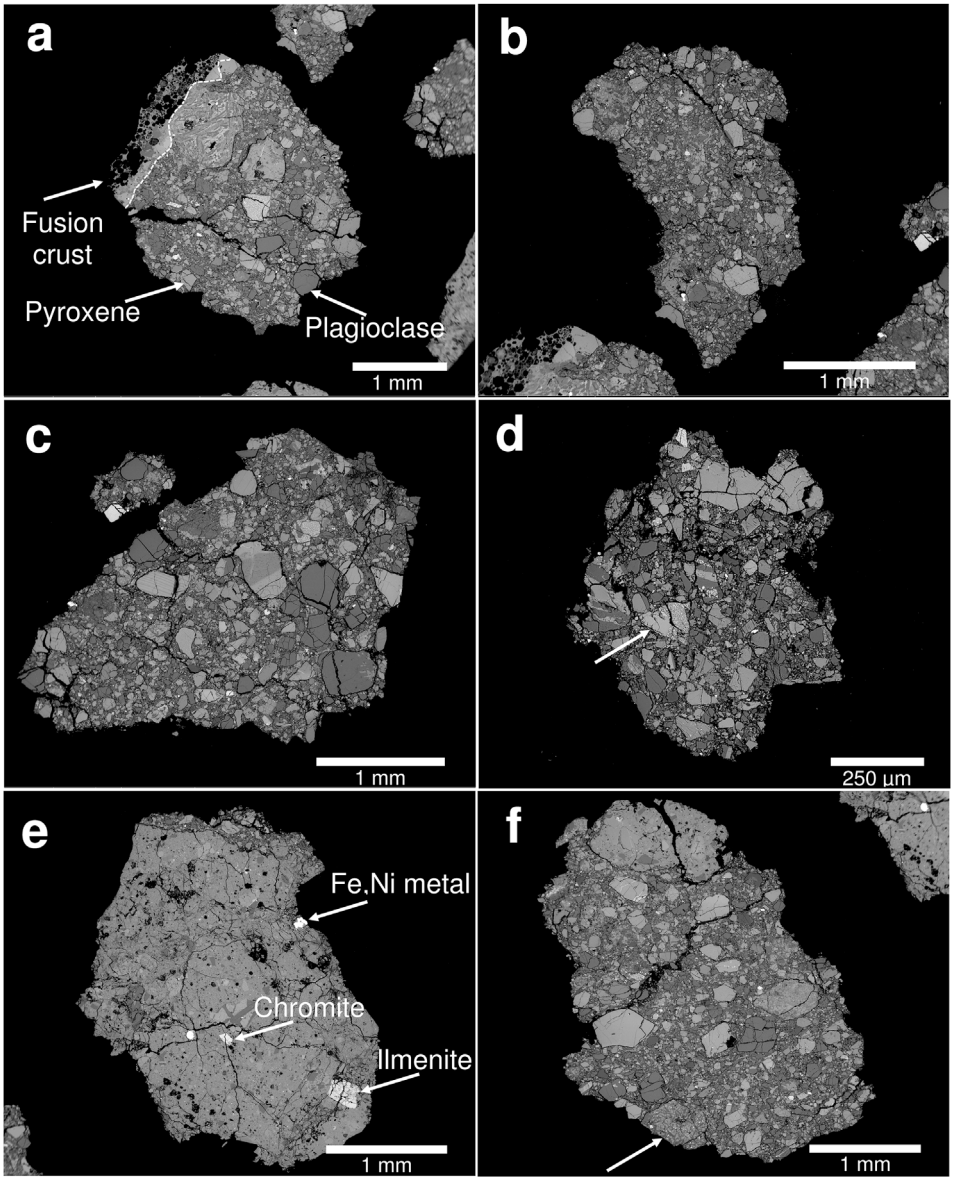

Fig. 3. Backscattered electron microscope images of Tintigny. The presence of different textures suggests Tintigny to be a brecciated eucrite. a) A sub-ophitic clast adjacent to the fusion crust shows a texture distinct from that of the host. In the center, a clast with a symplectitic texture is visible. b) Typical texture of Tintigny. A pyroxene with exsolution lamellae is visible. c) Variety of pyroxene textures including exsolution lamella and symplectitic assemblages. d) Partial transformation of pyroxene to a symplectitic assemblage is visible in one clast (shown by arrow). e) Dark grey clast (also visible in Fig. 2d), showing textural evidence of melt rock. f) The occurrence of different clasts. Note Fe-rich veins in a ~500 µm pyroxene in upper left. A clast with relatively larger crystals (shown with arrow) with similar sub-ophitic texture to the clast shown in 3a and 4e.

2. Methodology

Following examination of the whole rock using a stereomicroscope, representative fragments covering all petrographic textures were separated and embedded in resin at RBINS. Mineralogical and petrological studies were conducted using an optical microscope (ULB) and a PANalytical (Quanta 200) equipment Environmental Scanning Electron Microscope (ESEM) equipped with an EDAX (Apollo 10 silicon drift detector) Energy Dispersive Spectrometer (EDS) at the RBINS. The chemical composition of mineral phases were determined using a CAMECA SX50 electron microprobe (EMP) at the CAMPARIS facility (Paris), relying on a series of natural and synthetic standards and a later correction for SiO_2 calibration. The set instrument parameters include a focused electron beam (~1 µm in diameter), an accelerating voltage of 15 kV and a beam current of 10 nA. We aimed to analyze pyroxene and plagioclase with diverse compositions. Special care was considered to avoid grain boundaries, cracks etc. which can bias the quality of the analytical data. Whole-rock major and trace elemental concentrations were determined at the Laboratoire G-Time of the ULB, Belgium. Around 50 mg of sample representing the most common lithology (light grey) of the meteorite, was dissolved by alkaline fusion for major and trace element contents. Major elements were measured using a Thermo Fisher Scientific iCAP inductively coupled plasma-optical emission spectrometer (ICP-AES) at ULB with Y as an internal standard. Overall, the total reproducibility estimated based on United States Geological Survey reference material BHVO-2 is calculated to be better than 2% relative standard deviation (RSD). Trace elements were measured using the Agilent 7700 Quadrupole-Inductively Coupled Plasma-Mass Spectrometer (Q-ICP-MS) operated with a He-filled collision cell at ULB. Indium was used as internal standard. The total reproducibility estimated based on USGS reference material BHVO-2 is calculated to be better than 10% relative standard deviation (RSD).

High-precision oxygen isotopic analysis of Tintigny was undertaken at the Open University (Milton Keynes, UK) using an infrared laser-assisted fluorination system (Miller et al., 1999; Greenwood et al., 2017). Measurements were made on a 200 mg aliquot of silicates from the bulk sample. Approximately 2 mg aliquots of samples and standards were loaded into a nickel sample block, which was then placed in a two-part chamber, made vacuum tight using a compression seal with a copper gasket and quick-release KFX clamp (Miller et al., 1999). A 3 mm thick BaF_2 window at the top of the chamber allows simultaneous viewing and laser heating of samples. Prior to analysis the sample

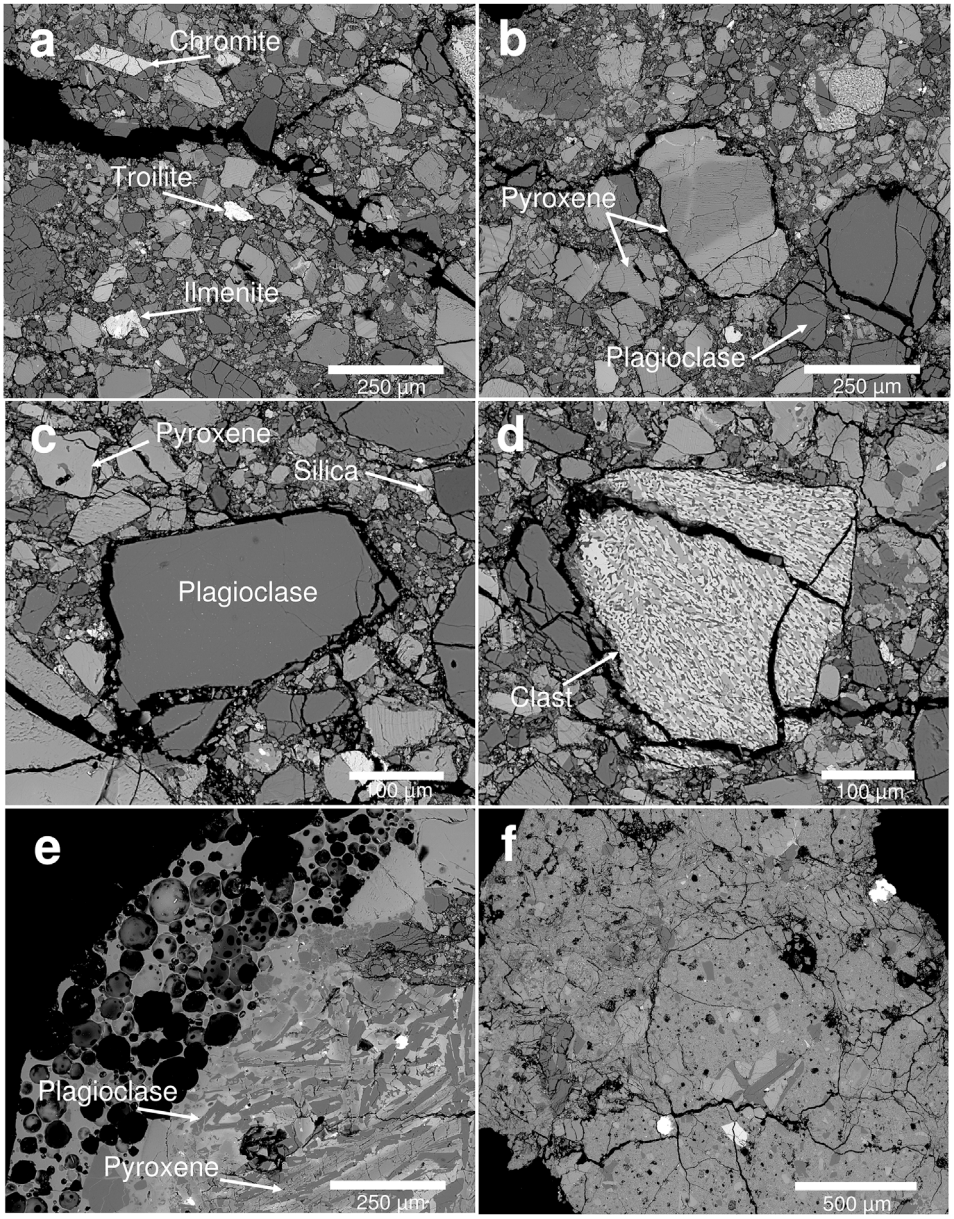

Fig. 4. a) Accessory minerals in Tintigny. b) Pyroxene showing a variety of textures (exsolution, twinning, symplectitic, etc.), suggesting a complex thermal history experienced by the Tintigny. c) Clastic texture of Tintigny formed as a result of impact metamorphism on the parent body surface. d) A symplectitic assemblage of hedenbergite-fayalite-silica. e) Alignment of plagioclase along the surface of pyroxene. Note the higher concentration of Fe in pyroxene rims. f) A closer view of the dark grey clast (Fig. 2d) shows lower number of crystals and a shock-melted texture.

chamber was heated overnight under vacuum to a temperature of about 70 °C to remove any adsorbed moisture. Following overnight heating, the chamber was allowed to cool to room temperature and was then flushed with several aliquots of BrF_5. The system was then left to pump for at least a further 24 h and oxygen isotopic analysis was only undertaken when the blank level reached <60 nmol of O_2. Sample heating in the presence of BrF_5 was carried out using a Photon Machines Inc. 50 W infrared CO_2 laser (10.6 µm) mounted on an X-Y-Z gantry. Reaction progress was monitored by means of an integrated video system. After fluorination, the released O_2 was purified by passing it through two cryogenic nitrogen traps and over a bed of heated KBr to remove any excess fluorine. The isotopic composition of the purified oxygen gas was analyzed using a Thermo Fisher MAT 253 dual inlet mass spectrometer with a mass resolving power of approximately 200.

Overall system precision, as defined by replicate analyses of our internal obsidian standard, is: ±0.053‰ for $\delta^{17}O$; ±0.095‰ for $\delta^{18}O$; ±0.018‰ for $\Delta^{17}O$ (2σ) (Starkey et al., 2016). Oxygen isotopic analyses are reported in standard δ notation, where $\delta^{18}O$ has been calculated as: $\delta^{18}O = [(^{18}O/^{16}O)_{sample}/(^{18}O/^{16}O)VSMOW -1]\ 1000$ (‰) and similarly for $\delta^{17}O$ using the $^{17}O/^{16}O$ ratio. VSMOW is the international standard Vienna Standard Mean Ocean Water. $\Delta^{17}O$, which represents the deviation from the terrestrial fractionation line, has been calculated using the linearized format of Miller (2002):

$$\Delta^{17}O = 1000\ln(1+(\delta^{17}O/1000)) - \lambda 1000\ln(1+(\delta^{18}O/1000)) \text{ where } \lambda = 0.5247.$$

3. Results

3.1. Macroscopic description

As a result of the thermal effects experienced during atmospheric entry and impact through the roof of the building, the Tintigny meteorite finally fragmented into several pieces during its extensive manual handling alongside fractures, indicated by the occurrence of broken surfaces. The single recovered fragment weighs 210 g (Fig. 2).

The meteorite is partly covered by a shiny black fusion crust, which varies in thickness depending on the morphology of the underlying

Table 1
The analyzed pyroxene and plagioclase compositions (in wt%) from Tintigny.

Mineral	Pyx #1	Pyx #2	Pyx #3	Pyx #4	Pyx #5	Pyx #6	Pyx #7	Pyx #8	Pyx #9	Pyx #10	Pyx #11	Pyx #12	Pyx #13	Pyx #14	Plg #1	Plg #2	Plg #3	Plg #4
SiO_2	52.57	52.53	52.64	49.91	51.26	49.09	51.03	49.27	49.81	53.01	46.09	47.68	49.81	45.54	47.20	48.20	45.55	50.14
Al_2O_3	1.70	0.61	0.83	0.59	0.82	0.68	0.94	1.24	0.81	1.15	1.98	0.97	1.04	1.17	32.25	33.23	34.16	31.01
TiO_2	0.26	0.15	0.11	0.39	0.51	0.42	0.20	0.47	0.71	0.15	1.11	0.74	0.67	0.92	0.00	0.00	0.01	0.03
FeO	20.87	27.24	23.95	32.26	17.91	32.54	23.61	27.97	28.50	20.46	32.58	31.56	23.21	37.84	0.63	0.57	0.51	0.63
Cr_2O_3	0.84	0.22	0.61	0.23	0.31	0.30	0.93	0.41	0.35	0.74	0.24	0.21	0.33	0.18	b.d.l.	b.d.l.	0.01	b.d.l.
MnO	0.76	0.74	0.86	1.06	0.45	0.91	0.85	0.88	0.88	0.74	0.87	0.82	0.75	1.03	b.d.l.	0.02	0.01	0.05
MgO	19.40	17.28	17.69	10.33	10.51	12.96	17.50	10.72	11.49	20.84	5.37	7.88	8.77	2.58	0.06	0.02	0.05	0.04
CaO	3.98	1.21	3.69	4.85	17.80	1.55	4.44	7.52	7.00	2.80	9.63	8.15	15.25	9.08	17.00	16.83	17.99	14.65
Na_2O	0.02	0.03	0.01	0.01	0.04	b.d.l.	0.01	0.07	0.07	b.d.l.	0.17	0.10	0.05	0.01	1.52	1.64	1.06	2.48
K_2O	b.d.l.	0.03	0.02	0.01	0.01	0.01	b.d.l.	0.02	0.02	0.01	0.01	0.05	0.01	b.d.l.	0.08	0.10	0.02	0.15
NiO	0.05	0.06	0.03	0.03	0.07	0.15	b.d.l.	0.08	0.03	0.01	0.04	b.d.l.	0.07	0.07	0.01	0.01	b.d.l.	0.05
Total	100.40	100.10	100.44	99.67	99.69	98.61	99.51	98.65	99.67	99.91	98.09	98.16	99.96	98.42	98.75	100.62	99.37	99.23
En (mol%)	57.1	51.7	52.4	32.4	31.5	40.1	51.6	33.7	35.3	60.7	17.6	25.1	26.8	8.5	–	–	–	–
Fs (mol%)	34.5	45.7	39.8	56.7	30.1	56.5	39.0	49.3	49.2	33.4	59.8	56.3	39.8	70.0	–	–	–	–
Wo (mol%)	8.4	2.6	7.9	10.9	38.4	3.4	9.4	17.0	15.5	5.9	22.6	18.6	33.5	21.5	–	–	–	–
Fe/Mn	27.1	36.3	27.5	30.1	39.3	35.3	27.4	31.4	32.0	27.3	37.0	38.0	30.6	36.3	–	–	–	–
Fe/Mg	0.6	0.9	0.8	1.7	1.0	1.4	0.8	1.5	1.4	0.6	3.4	2.2	1.5	8.2	–	–	–	–
An (mol%)	–	–	–	–	–	–	–	–	–	–	–	–	–	–	85.7	84.5	90.3	75.8
Ab (mol%)	–	–	–	–	–	–	–	–	–	–	–	–	–	–	13.8	14.9	9.6	23.2
Or (mol%)	–	–	–	–	–	–	–	–	–	–	–	–	–	–	0.5	0.6	0.1	0.9

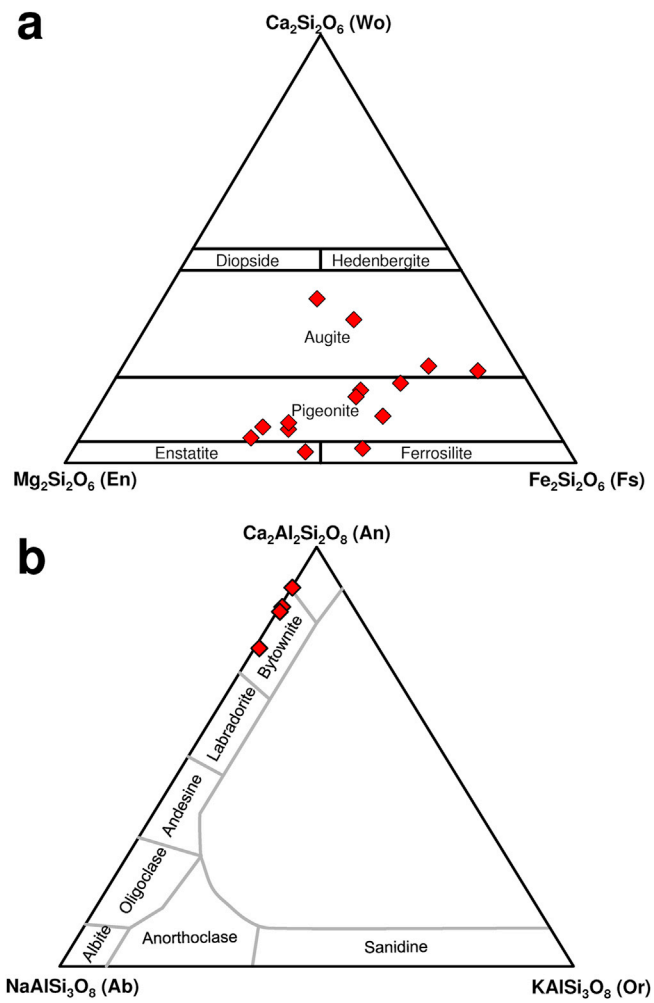

Fig. 5. Pyroxene and plagioclase compositions in Tintigny.

surface. Three main varieties of fusion crust are present: (i) the thickest (~1–2 mm) parts that occur in hollow areas of the surface and display a wavy texture comprising elevated ribbons of molten material (flow lines) (Fig. 2a); (ii) the main part that is considerably thinner (~0.5 mm) and indicates a full layer of molten material with a texture containing assemblages of crater-like pits (Fig. 2b); (iii) the intermediate part exhibiting a combination of these two variations, with a patchy texture occurring along the edges of the meteorite surface. Several cracks occur on the surface of the fusion crust. They correspond to deeper fractures visible where the surface is broken (Fig. 2c). At these sites, a light grey interior is revealed, composed of a fine-grained light-colored matrix hosting darker crystals and a cm-size dark grey clast (Fig. 2d). Macroscopic observations indicate that Tintigny is a brecciated achondrite.

3.2. Microscopic description

Using optical and electron microscopy, Tintigny exhibits a brecciated sub-ophitic basaltic texture mainly composed of plagioclase/maskelynite and clinopyroxene (Fig. 3). These minerals occur both as large crystals (>50 μm) and as smaller (<50 μm) ones, the latter mainly composing the clastic matrix. Accessory minerals include troilite, ilmenite, chromite, (Fe,Ni) metal, and silica. Most of the minerals exhibit well-delineated edges, enhancing the clastic texture of the rock. At least two generations of shock fractures are visible: those specific to clasts and large crystals, and those cross-cutting both the larger grains and the matrix materials.

In addition to the main sub-ophitic texture, at least three distinct

Table 2
Major and trace element composition of Tintigny eucrite. Concentrations are reported in mg/g and μg/g for major and trace elements, respectively.

	Tintigny	RSD (%)	BHVO-2[a]	RSD (%)	BVHO-2[b]
Na	3.26	2	16.0	0.7	16.4
Mg	46.1	1	43.5	2	43.6
Al	63.0	0.8	71.7	0.5	71.6
Si	229	1	235	0.4	233
P	0.206	1	1.17	2	1.2
K	0.339	0.6	4.29	0.8	4.30
Ca	68.3	0.7	81.3	1	81.7
Ti	3.78	1	16.4	1	16.3
Cr	2.73	0.4	0.315	1	0.280
Mn	4.21	1	1.33	1	1.3
Fe	142.3	1	89.1	0.4	86.3
Ga	2.63	12	22.57	1	21.7
Rb	0.351	49	8.35	5	9.80
Sr	79.7	1	394	1	389
Y	19.0	1	25.2	0.4	28.0
Zr	49.6	1	162	1	172
Nb	4.34	2	17.2	1	18
Ba	34.4	2	134	1	130
La	4.65	3	16.0	1	15.2
Ce	10.5	0	37.6	1	38.0
Pr	1.51	4	5.25	2	5.34
Nd	7.04	3	24.1	3	25.0
Sm	2.09	5	6.18	4	6.20
Eu	0.660	2	2.10	2	2.07
Gd	2.91	2	6.40	3	6.30
Tb	0.490	2	0.910	1	0.940
Dy	3.32	2	5.34	2	5.31
Ho	0.727	1	0.994	3	1.04
Er	2.08	4	2.52	4	2.54
Tm	0.310	3	0.337	8	0.335
Yb	1.99	3	2.00	2	2.00
Lu	0.280	11	0.274	7	0.280
Hf	1.39	2	4.32	4	4.47
Ta	0.270	10	1.22	2	1.40
Th	0.441	6	1.17	2	1.25
U	0.121	3	0.407	5	0.412
Pb	0.162	17	0.769	1	1.65

[a] BHVO-2 basalt reference material analyzed during same session.
[b] Compilled literature value from GeoReM database (http://georem.mpch-mainz.gwdg.de/).

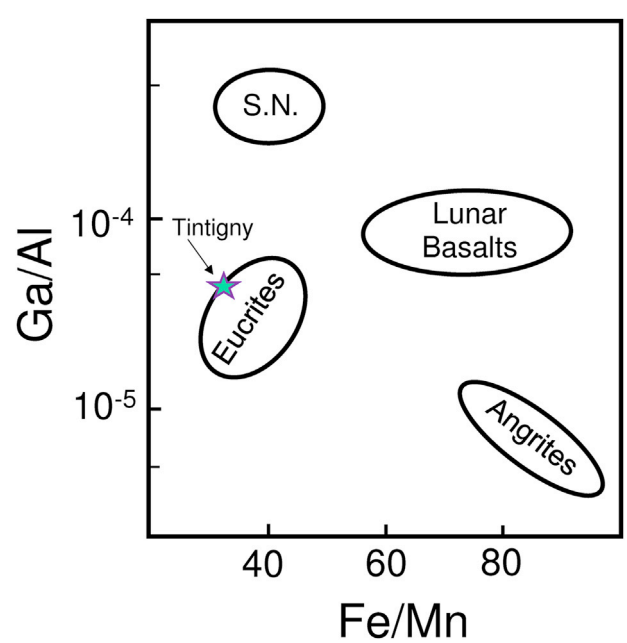

Fig. 6. Ga/Al vs. Fe/Mn of Tintigny in comparison to other basaltic meteorites. Plot modified from Barrat et al. (2003). S.N. stands for shergottites and nakhlites clan of Martian meteorites.

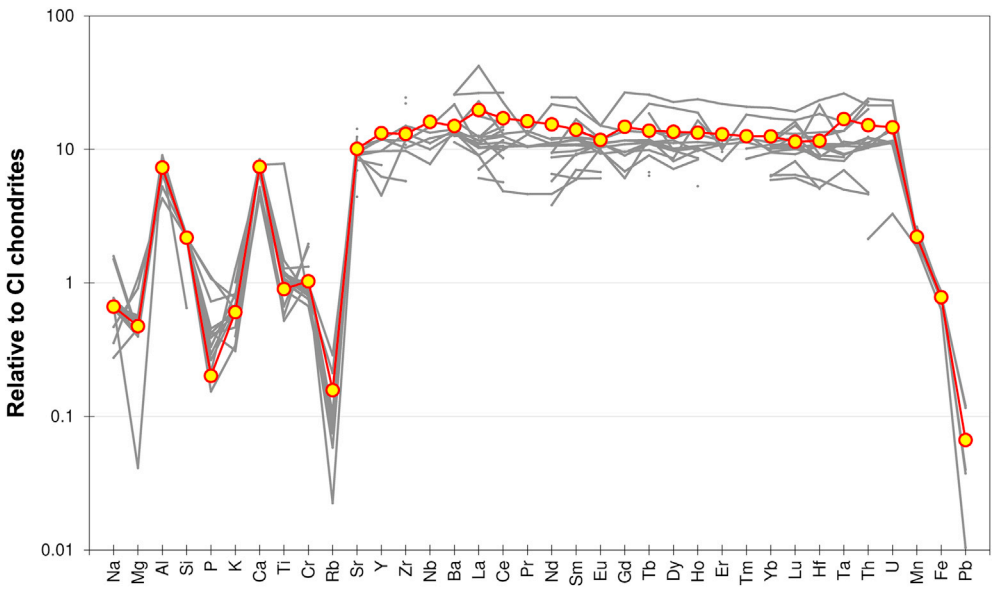

Fig. 7. CI-normalized whole-rock chemical composition of Tintigny and 18 noncumulate eucrites (Béréba, Bouvante, Cachari, Chervony Kut, Elephant Moraine A79004,A79005, Haraiya, Ibitira, Junzac, Juvinas, Millbillillie, Moore County, Pasamonte, Pomozdino, Yamato 794002,791573,82049,82202). Eucrite data from Kitts and Lodders (1998), Mittlefehldt (2015). Average CI chondrite data are from Wasson and Kallemeyn (1988). Lithophile, siderophile, and chalcophile elements are shown with increasing atomic number, respectively.

textures are present in specific clasts. These clasts are different from their host based on their texture and degree of equilibrium recorded in the composing minerals. Figs. 3a and 4e shows a ~1 mm long clast with a sub-ophitic texture. Elongated pyroxenes are unequilibrated and display Fe enriched rims. The elongation directions of pyroxene crystals control the alignment of plagioclase. Abundant cracks perpendicular to pyroxene elongation are visible. They are absent from the adjacent plagioclase crystals, suggesting elevated levels of mechanical stress prior plagioclase crystallization. Some of these plagioclase crystals are cut by randomly oriented cracks, which are filled by Fe-rich pyroxenes. This is related to fusion crust formation. Another clast with a similar texture is visible in Fig. 3f.

Under the electron microscope, the dark clast visible on the broken surface (Fig. 2d) displays a melt rock texture (Figs. 3e and 4f). The groundmass is a mixture of quenched pyroxene and plagioclase and only a few larger grains including (Fe,Ni) metal, ilmenite, chromite, and an intergrowth of plagioclase-pyroxene are present.

A single ~0.5 mm clast and several smaller grains exhibit a symplectitic mixture of pyroxene, fayalite, and silica (Fig. 3a,c,d and Fig. 4b,d).

A small number of pyroxenes show evidence of Fe enrichment along veins and crystal rims (Figs. 3f and 4b,e). These fractures are mostly limited to individual grains and do not occur in the whole rock, indicating their formation was prior to the assembly of Tintigny on its parent body.

3.3. Mineral chemistry

Table 1 summarizes the chemical composition of pyroxene and plagioclase crystals analyzed randomly in different fragments of Tintigny. Mineral chemistry calculations of pyroxene end members show ranges from 8.5 to 60.7 mol% for enstatite, 30.1–70.0 mol% for ferrosilite, and 2.6–38.4 mol% for wollastonite. Based on these values, most pyroxenes in Tintigny are pigeonite and augite (Morimoto, 1988; Marshall, 1996) (Fig. 5a). The Fe/Mn ratios of pyroxenes range from 27.1 to 39.3, with the highest ratio observed in pyroxene from the symplectitic clast (Pyx #5, Table 1). Fe/Mn and Fe/Mg ratios in low-Ca pyroxene (Wo < 10, Pyx #1,2,3,6,7,10) are 30.2 ± 4.4 and 0.8 ± 0.3, respectively. These ratios in high-Ca pyroxene (n = 8) are 34.3 ± 3.7 for Fe/Mn and 2.6 ± 2.4 for Fe/Mg. The average pyroxene Fe/Mn ratio for all pyroxene is 32.5 ± 4.4 (SD, n = 14). Fe/Mg ranges from 0.6 to 8.2, with an average value of 1.8 ± 2.0 (SD, n = 14). Considering pyroxene Fe/Mn ranges of 40 ± 11, 62 ± 18, 32 ± 6, and 30 ± 2 for basaltic rocks from the Earth, Moon, Mars, and 4 Vesta (eucrites), respectively, and based on our data, particularly those of low-Ca pyroxene, Tintigny falls in the range of basaltic eucrites (Papike et al., 2003). We believe the higher standard deviation of our data results from a higher diversity and relatively lower number of the analyzed minerals.

The anorthite content of four analyzed plagioclase ranges from 75.8 to 90.3 mol%. Plagioclase in the symplectitic clast, with 75.8 mol% anorthite, is less calcic (and more sodic) than the host (Fig. 5b). Excluding this clast, the anorthite percentage averages to 86.8 ± 3.4 mol % (SD, n = 3). This value is in range of both vestan (87 ± 2 mol%) and lunar rocks (89 ± 3 mol%) (Papike et al., 2003), however the Fe/Mn ratio of pyroxene indicates that Tintigny is a member of the HED suit.

3.4. Whole-rock chemical composition

Table 2 shows the major and trace element concentrations of Tintigny. Based on bulk rock Fe/Mn vs. Fe/Mg ratios, three distinct zones for chondrites, lunar rocks, and howardite-eucrite-diogenite (HED)/Martian meteorites can be defined (Goodrich and Delaney, 2000). For Tintigny, the bulk rock Fe/Mn and Fe/Mg ratios are 33.9 and 3.1, respectively. These values overlap with those measured for HED and Martian meteorites. To discriminate between different types of basaltic achondrites, Fe/Mn has previously been combined with other useful ratios such as Ga/Al (Barrat et al., 2003). The Ga/Al ratio of Tintigny is 4.17×10^{-5}, fully in range of those of eucrites (Fig. 6). The CI-normalized elemental concentrations for Tintigny are compared to those of 18 noncumulate eucrites in Fig. 7. The latter plot indicates the strong similarities between the chemical composition of Tintigny and that of noncumulate eucrites. This similarity to eucrites is also evident based on various combinations of major and trace elements for HED. On a binary plot of Ca versus Mg, Tintigny overlaps with eucrites, but is distinct from howardites or diogenites (Fig. 8). Similar behavior occurs in Sm versus Mg and Yb versus La plots. Based on the abundance of TiO_2 (0.63%) and FeO/MgO ratio (2.66), Tintigny is a member of non-cumulate eucrites (Fig. 9) (Barrat et al., 2003).

3.5. Oxygen isotopic composition

Two replicate analyses Tintigny gave the following oxygen isotopic: $\delta^{17}O$ = 1.723 ± 0.018 (1σ); $\delta^{18}O$ = 3.756 ± 0.041 (1σ) and $\Delta^{17}O$ = −0.246 ± 0.003 (1σ). The oxygen isotope data for Tintigny are

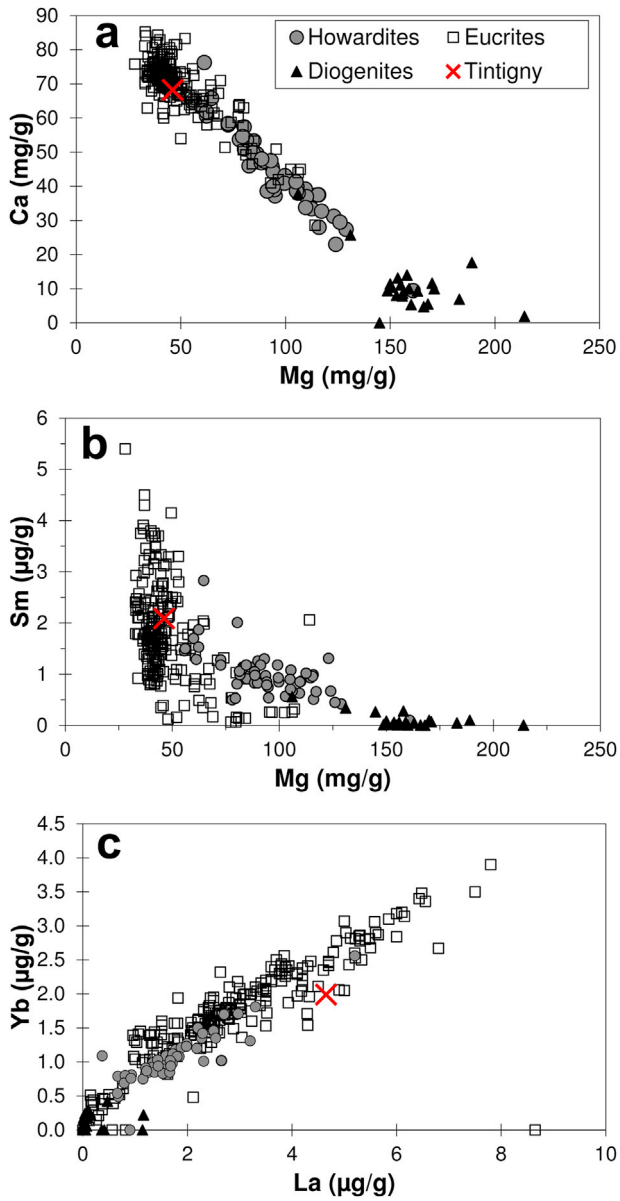

Fig. 8. The abundance of Mg vs. Ca, Mg vs. Sm., and La vs. Yb for Tintigny in relation to howardite-eucrite-diogenite (HED) meteorites. Compilation of HED data by Mittlefehldt (2015).

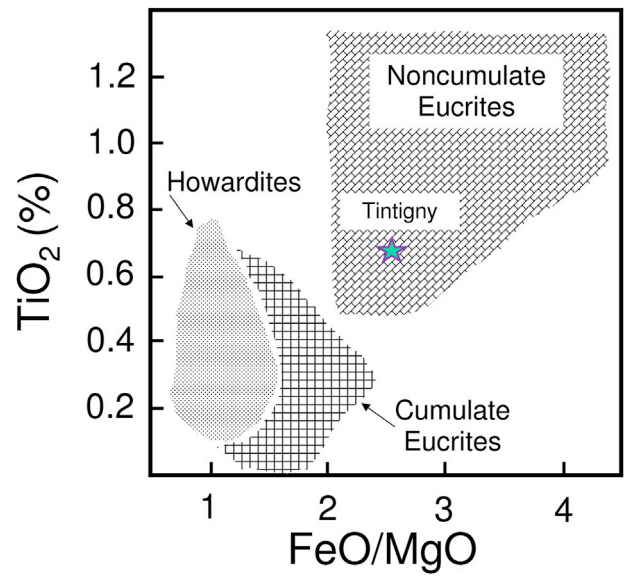

Fig. 9. TiO_2 vs. FeO/MgO of Tintigny in comparison to howardite and eucrites. Plot modified from Barrat et al. (2003).

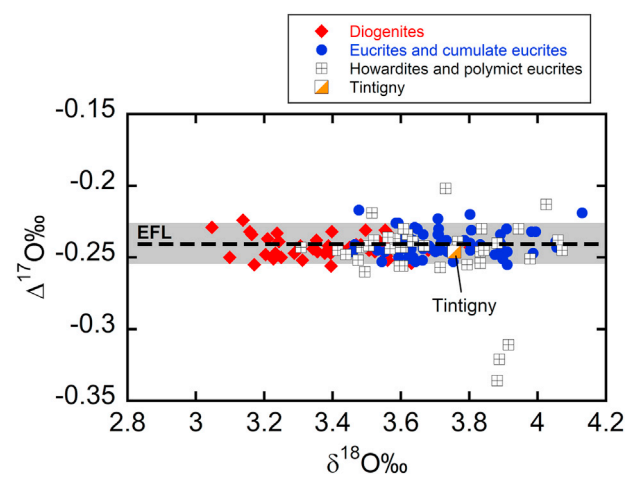

Fig. 10. Oxygen isotopic composition of Tintigny in comparison with HED meteorites. HED data from Greenwood et al. (2017).

plotted in relation to the HED data of Greenwood et al. (2017) in Fig. 10 and this shows that the meteorite lies close to the Eucrite Fractionation Line (EFL) defined by eucrite and diogenite falls ($\Delta^{17}O = -0.240$). In addition, the $\delta^{18}O$ value of Tintigny plots centrally in the field of eucrite analyses. The oxygen isotopic data is therefore consistent with the classification of Tintigny as a eucrite.

4. Discussion and conclusions

In this work, we used petrography, mineralogy, and whole-rock major and trace-element chemistry to classify the Tintigny meteorite. In addition, we have undertaken oxygen isotope analysis which has confirmed that Tintigny is a member of the HED clan. Based on our studies we conclude that Tintigny is a non-cumulate eucrite, specifically a polymict basaltic eucrite.

Eucrites, together with howardites and diogenites, form the HED clan that constitutes 74.6% by number of all achondrites, and 3.6% by number of all meteorites in meteorite collections worldwide (Meteoritical Bulletin Database (https://www.lpi.usra.edu/meteor/metbull.php), accessed August 2021). Based on the spectral data obtained in the laboratory and their comparison with data measured by ground-based observatories and the results from the NASA Dawn mission, HEDs are thought to originate from differentiated asteroids with V-type spectra, and in particular 4 Vesta (McSween et al., 2010; Moskovitz et al., 2010). Postcrystallization events on the parent body such as thermal metamorphism, metasomatism, shock metamorphism, and space weathering have led to the formation of rocks with complex geological histories (Yamaguchi et al., 1994; Takeda and Mori, 1985; Warren et al., 2014). As described earlier, Tintigny has also been affected by these processes, in particular thermal and shock metamorphism and possibly metasomatism as recorded in some grains (as Fe enrichment along veins and crystal rims). Many HED meteorites are brecciated, with a general distinction between monomict and polymict breccias (Delaney and Prinz, 1984; Mittlefehldt et al., 2013; Zucolotto et al., 2019). These breccias result

from large-scale impact events of the Solar System bodies and witness to the importance of impact processing of the surface and subsurface of planetary bodies. The lack of chemical zoning in most minerals (except in some clasts), the presence of Fe, Ni metal exsolutions in pyroxene, and sub-solidus exsolution of augite lamellae within pigeonite hosts (Fig. 4) are indicative of parent body thermal metamorphism (Righter and Drake, 1997; Vollmer et al., 2020). The formation of clasts with symplectitic texture has been suggested to result from the breakdown of metastable pyroxene in gabbroic eucrites (Patzer and McSween, 2012; Seddiki et al., 2013). Barrat et al. (2011) and Warren et al. (2014) linked the formation of Fe enrichment along the veins and crystal rims to fluid-driven alteration on the parent body surface.

Diogenites are mostly orthopyroxene cumulates that formed in plutons which crystallized at varying levels within the crust. Eucrites are mostly basaltic rocks that formed at faster cooling rates, most likely as a result of emplacement either on the surface or at shallow depths. According to their textural and compositional characteristics eucrites can be further divided into basaltic rocks (mostly monomict breccias), cumulate gabbros, and polymict eucrites made of different eucritic textures (without diogenitic clasts) like Tintigny (Vollmer et al., 2020). Barrat et al. (2003) also divides them to cumulate and noncumulate eucrites. Howardites formed as the products of impact events on the parent body surface, occurring as breccias made from different percentages of eucritic and diogenitic materials.

Meteoritical Bulletin Database (https://www.lpi.usra.edu/meteor/metbull.php; August 2021) lists 2447 HED meteorites encompassing 1516 eucrites, 399 howardite, and 532 diogenites. Out of this number, only 69 of the HED are *falls,* i.e., meteorites that have been observed falling and have been collected soon after their impact, avoiding the detrimental effects of terrestrial weathering, which are common in meteorite *finds* (meteorites without any fall record) and even in some cases in *falls* if not collected immediately (Walker et al., 2018; Pourkhorsandi, 2018; Pourkhorsandi et al., 2019). Including Tintigny, only 39 eucrite falls are known to date, 11 of them occurred in Europe and Tintigny being the only one from Belgium. This highlights the importance of classification and accessibility of such a meteorite for further cosmochemical and planetary studies and enriching our knowledge on the formation of HED meteorites and their parent bodi(es). In addition to its scientific importance, we emphasize the importance of the discovery of a historical meteorite fall in bringing attention to national scientific heritage that has to be properly understood and safeguarded for the generations of scientists, scholar, and amateurs to come (Franza and Pratesi, 2021).

Authorship statement

All persons who meet authorship criteria are listed as authors, and all authors certify that they have participated sufficiently in the work to take public responsibility for the content, including participation in the concept, design, analysis, writing, or revision of the manuscript. Furthermore, each author certifies that this material or similar material has not been and will not be submitted to or published in any other publication before its appearance in the Planetary and Space Science journal.

Declaration of competing interest

The authors declare that they have no known competing financial interests or personal relationships that could have appeared to influence the work reported in this paper.

Acknowledgments

We all warmly thank the Schmitz family for their donation of the meteorite to the RBINS. We thank W. Debouge, S. Cauchies, and J. de Jong for their support in the clean labs and analysis facilities at the Laboratoire G-Time. We appreciate constructive comments by the two anonymous reviewers and editorial handing by Dr. A.P. Rossi.

This project has received funding from the European Union's Horizon 2020 research and innovation programme under the Marie Skłodowska-Curie grant agreement No 801505. VD thanks the ERC StG "ISoSyC" and FRS-FNRS for funding. SG, SD and VD thank the Brain-be Belspo projects BAMM and DESIRED for funding.

References

Barrat, J.A., Jambon, A., Bohn, M., Blichert-Toft, J., Sautter, V., Gopel, C., Gillet, Ph, Boudouma, O., Keller, F., 2003. Petrology and geochemistry of the unbrecciated achondrite Northwest Africa 1240 (NWA 1240): an HED parent body impact melt. Geochem. Cosmochim. Acta 67, 3959–3970.

Barrat, J.A., Yamaguchi, Y., Bunch, T.E., Bohn, M., Bollinger, C., Ceuleneer, G., 2011. Possible fluid-rock interactions on differentiated asteroids recorded in eucritic meteorites. Geochem. Cosmochim. Acta 75, 3839–3852.

Delaney, J.S., Prinz, M., 1984. The polymict eucrites. J. Geophys. Res. 89 (S01), C251–C288. https://doi.org/10.1029/JB089iS01p0C251.

Franza, A., Pratesi, G., 2021. Meteorites as a scientific heritage. Conservar Património 36, 106–121.

Gattacceca, J., McCubbin, F.M., Bouvier, A., Grossman, J., 2020. The meteoritical Bulletin No. 107. Meteoritics Planet Sci. 55, 460–462.

Goodrich, C., Delaney, J., 2000. Fe/Mg-Fe/Mn relations of meteorites and primary heterogeneity of primitive achondrite parent bodies. Geochem. Cosmochim. Acta 64, 149–160.

Greenwood, R.C., Burbine, T.H., Miller, M.F., Franchi, I.A., 2017. Melting and differentiation of early-formed asteroids: the perspective from high precision oxygen isotope studies. Chemie der Erde-Geochem. 77, 1–43.

Kitts, K., Lodders, K., 1998. Survey and evaluation of eucrite bulk compositions. Meteoritics Planet Sci. 33, A197–A213.

McSween, H.Y., Mittlefehldt, D.W., Beck, A.W., Mayne, R.G., McCoy, T.J., 2010. HED meteorites and their relationship to the geology of Vesta and the Dawn mission. In: Russell, C., Raymond, C. (Eds.), The Dawn Mission to Minor Planets 4 Vesta and 1 Ceres. Springer, New York, NY.

Miller, M.F., Franchi, I.A., Sexton, A.S., Pillinger, C.T., 1999. High precision $\Delta^{17}O$ isotope measurements of oxygen from silicates and other oxides: methods and applications. Rapid Commun. Mass Spectrom. 13, 1211–1217.

Miller, M.F., 2002. Isotopic fractionation and the quantification of ^{17}O anomalies in the oxygen three-isotope system: an appraisal and geochemical significance. Geochem. Cosmochim. Acta 66, 1881–1889.

Mittlefehldt, D.W., Herrin, J.S., Quinn, J.E., Mertzman, S.A., Cartwright, J.A., Mertzman, K.R., Peng, Z.X., 2013. Composition and petrology of HED polymict breccias: the regolith of (4) Vesta. Meteoritics Planet Sci. 48, 2105–2134.

Mittlefehldt, D.W., 2015. Asteroid (4) Vesta: I. The howardite-eucrite-diogenite (HED) clan of meteorites. Chemie der Erde - Geochem. 75, 155–183.

Marshall, D., 1996. Ternplot: an excel spreadsheet for ternary diagrams. Comput. Geosci. 22, 697–699.

Morimoto, N., 1988. Nomenclature of pyroxenes. Mineral. Petrol. 39, 55–76.

Moskovitz, N.A., Willman, M., Burbine, T.H., Binzel, R.P., Bus, S.J., 2010. A spectroscopic comparison of HED meteorites and V-type asteroids in the inner Main Belt. Icarus 208, 773–788.

Papike, J.J., Karner, J.M., Shearer, C.K., 2003. Determination of planetary basalt parentage: a simple technique using the electron microprobe. Am. Mineral. 88, 469–472.

Patzer, A., McSween, H.Y., 2012. Ordinary (mesostasis) and not-so-ordinary (symplectites) late-stage assemblages in howardites. Meteoritics Planet Sci. 47, 1475–1490.

Pourkhorsandi, H., 2018. Meteorites of Iran and hot deserts: classification and weathering.. PhD Thesis, Aix-Marseille Université, Marseille (France), p. 202.

Pourkhorsandi, H., Gattacceca, J., Rochette, P., D'Orazio, M., Kamali, H., de Avillez, R., Letichevsky, S., Djamali, M., Mirnejad, H., Debaille, Jull, A.J.T., 2019. Meteorites from the Lut Desert (Iran). Meteoritics Planet Sci. 54, 1737–1763.

Righter, K., Drake, M.J., 1997. A magma ocean on Vesta: core formation and petrogenesis of eucrites and diogenites. Meteoritics Planet Sci. 32, 929–944.

Seddiki, A., Moine, B., Cottin, J.Y., Bascou, J., Godard, M., Faure, F., Bourot-Denise, M., Remaci, N., 2013. A mineralogical and geochemical study of polymict eucrite discovered in Sahara of southwest Algeria. Arab. J. Geosci. 6, 3175–3184.

Starkey, N.A., Jackson, C.R.M., Greenwood, R.C., Parman, S., Franchi, I.A., Jackson, M., Fitton, J.G., Stuart, F.M., Kurz, M., Larsen, L.M., 2016. Triple oxygen isotopic composition of the high $^{3}He/^{4}He$ mantle. Geochem. Cosmochim. Acta 176, 227–238.

Takeda, H., Mori, H., 1985. The polymict eucrites. 1985. The diogenite-eucrite links and the crystallization history of a crust of their parent body. J. Geophys. Res. 90, C636–C648.

Vollmer, C., Rombeck, S., Roszjar, J., Sarafian, A.R., Klemme, S., 2020. The brecciated texture of polymict eucrites: petrographic investigations of unequilibrated meteorites from the Antarctic Yamato collection. Meteoritics Planet Sci. 55, 558–574.

Walker, R., Yin, Q., Heck, P., 2018. Rapid effects of terrestrial alteration on highly siderophile elements in the Sutter's Mill meteorite. Meteoritics Planet Sci. 53, 1500–1506.

Warren, P.H., Rubin, A.E., Isa, J., Gessler, N., Ahn, I., Choi, B., 2014. Northwest Africa 5738: multistage alteration in an extraordinarily evolved eucrite. Geochem. Cosmochim. Acta 141, 199–227.

Wasson, J., Kallemeyn, G., 1988. Compositions of chondrites. Phil. Trans. Math. Phys. Eng. Sci. 325, 535–544.
Yamaguchi, A., Takeda, H., Bogard, D.D., Garrison, D., 1994. Textural variations and impact history of the Millbillillie eucrite. Meteoritics 29, 237–245.
Zucolotto, M.E., Tosi, A.A., Villaca, C.V.N., Moutinho, A.L.R., Andrade, D.P.P., Faulstich, F., Gomes, A.M.S., Rios, D.C., Rocha, M.C., 2019. Serra Pelada: the first Amazonian meteorite fall is a Eucrite (basalt) from asteroid 4-Vesta. An Acad. Bras Ciências 90, 3–16.